Expansion test with one unload-reload loop and pore pressure measurement, first interpretation of dissipation tests, Larivot site

Vincent Savatier[1], *Philippe* Reiffsteck[2], *Antoine* Philippe[1] and *Michael* Peronne [3]

[1] *EGIS Geotechnique 33-43 avenue Georges Pompidou 31131 Balma, France*
[2] *Université Gustave Eiffel, GERS-SRO, 14-20 Blvd Newton, Cité Descartes, Champs sur Marne, 77447, France*
[3] *Jean Lutz SA, 2 rue du Forbeth, 64110 Jurançon, France*
[#]*Corresponding author: philippe.reiffsteck@univ-eiffel.fr*

ABSTRACT

This paper presents an interpretation of cyclic pressuremeter tests with pore pressure measurement performed at Larivot bridge site (French Guyana). In cohesive soils, test results are in accordance with the pressuremeter theory. The times at 50% dissipation correlate closely with those obtained from dissipation tests performed using a piezocone in the immediate vicinity.

Keywords: expansion test; pressuremeter, pore pressure; dissipation tests; correlation; CPT.

1. Introduction

Experience gained during piezocone tests has shown that measuring pore pressures during in situ tests is one of the ways of improving understanding and access to soil parameters (Lunne et al., 1997). In this paper, we present the interpretation of tests carried out on the Larivot site, as described in Reiffsteck et al. (2022), in the light of new in situ tests and settlement monitoring.

2. Behaviour of the soil during the test

2.1. PMTu device

This 32 m deep borehole, comprising 21 pressuremeter tests with pore pressure measurements (PMTu) positioned between 8 and 30.5 m, was drilled using the equipment developed by Jean Lutz SA (Figure 1a and b), (Karagiannopoulos et al., 2019; 2020). Figure 1a shows the architecture of the equipment used and its implementation in the field. A B2-ML1 box containing the analogue-to-digital conversion module acquires the signals from the pore pressure sensor positioned on the probe and the signals from the pressure sensors placed upstream of the solenoid valves of the Prevo automatic pressure meter to measure when these are closed. It also contains the power supply module. The signals are transmitted to the PC via a USB port. The PilotPrevo software records these measurements and sends instructions to the Prevo. Pore water pressure is measured mid-height up the probe using one or more sensor and its on-board electronic circuit, which are attached to the membrane of the flexible probe or the lamellae of the slotted tube (Figure 1b). A flexible membrane probe was used in the clayey layers and a slotted tube for the underlying materials.

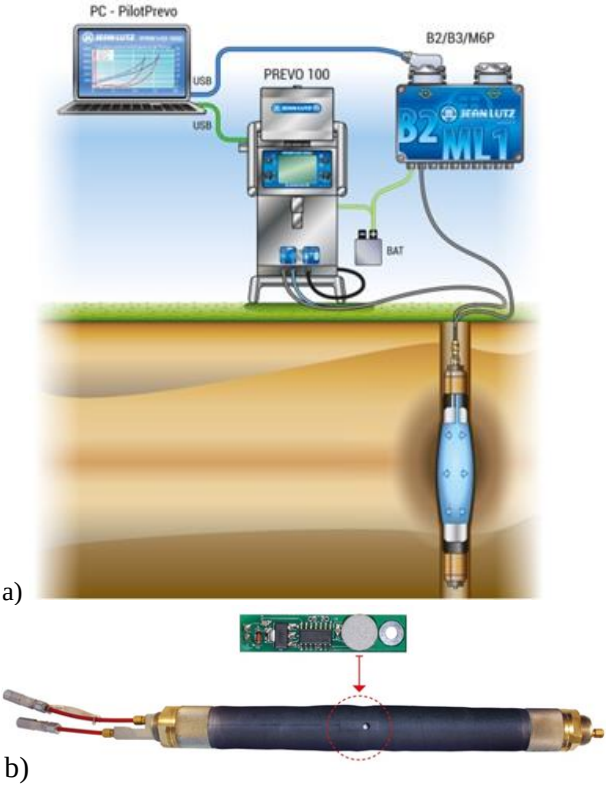

Figure 1. measurement system (a) complete apparatus (b) probe with pore water measurement transducer

This system allows reliable measurement of pore pressure variations in contact with the soil during a conventional test.

2.2. Testing program

Figure 2 summarizes the general principle of a test consisting of a first phase of pressure increase in steps

respecting the EN ISO 22476-5 standard (contact phase noted 1, pseudo-elastic phase noted 2, unloading phase rated 3 and reloading phase rated 4) followed by a dissipation phase at constant volume, initiated at an initial pressure close to $1{,}2 \cdot p_f$. The test ends with an unloading fifth phase.

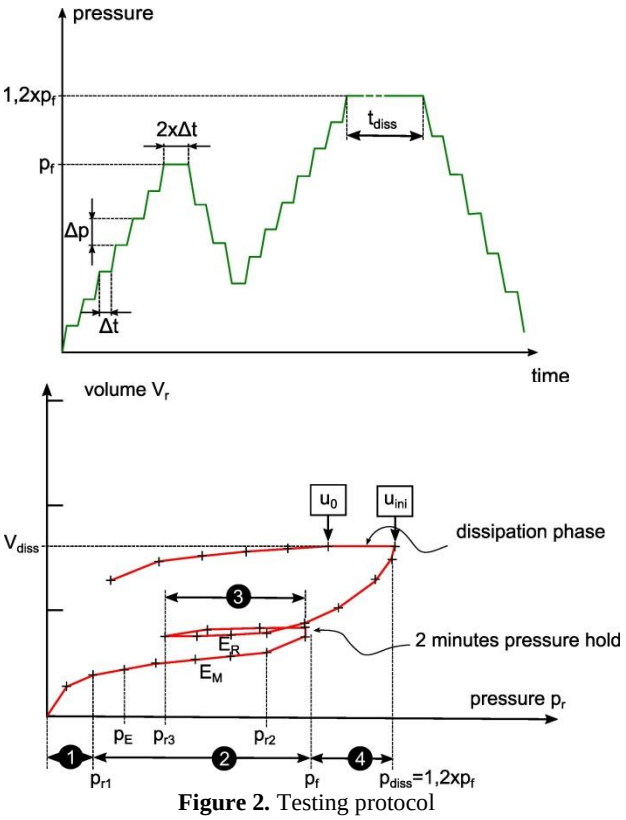

Figure 2. Testing protocol

The notations used in this figure are:
p_{r1}: pseudo-elastic phase first pressure;
p_f : creep pressure;
p_{r2}: pressure at the end of the elastic phase;
p_{r3}: pressure at the beginning of the reloading phase
p_E: first pressure of the segment used to derive E_M;
E_M: Ménard modulus according to EN ISO 22476-4;
E_R: reloading module;
u_{ini}: pore pressure measured at the closing of the valve;
u_0: hydrostatic pore pressure measured or estimated.

The unload-reload loop (numbered 3) was designed as follows:

$$p_{r3} = p_f - \frac{3}{4} \cdot (p_{r2} - p_{r1}) \quad (1)$$

rather than totally unloading the ground:

$$p_{r3} = p_E \quad (2)$$

2.3. Tests results on Larivot site

Rotational drilling using a 63 mm button tricone was used to pre-bore the cavity. The first 8 meters were directly cased in 104/113 mm with water as drilling fluid. Drilling stages of 2 m were favoured in the clay horizon and 5 m in the following horizon.

At the end of each drilling stage, a bentonite fluid was circulated for about a hundred liters to stabilize the cavity.

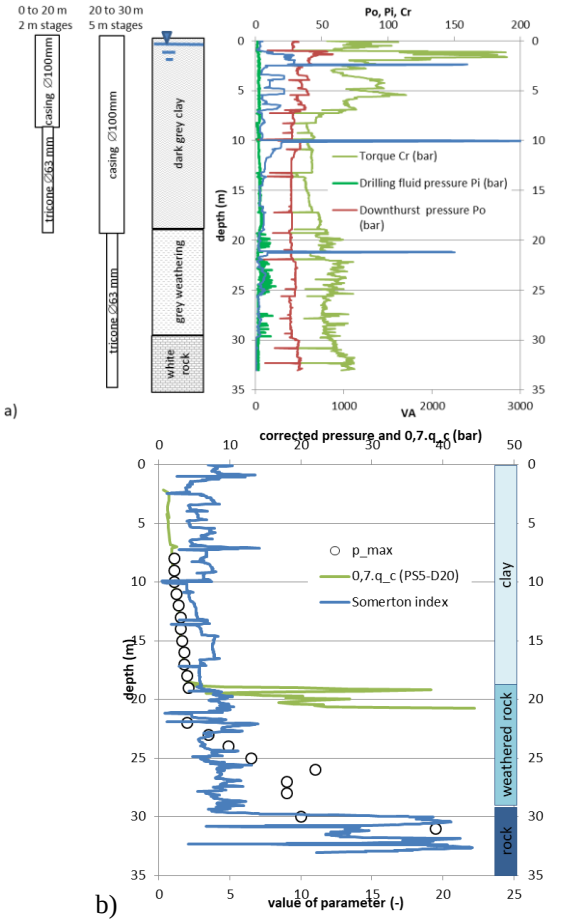

Figure 3. Profiles of (a) cavity embodiment, drilling parameters and (b) parameters derived from pressuremeter (p_{max}), CPT and drilling parameters

The ground investigation campaign included static cone penetrometer tests with dissipation tests. Figure 3a shows the drilling parameters obtained during the tests and the maximum pressure reched during expansion test ($p_{max} \cong p_\ell$). The Somerton index $I_s = P_o/\sqrt{V_a}$ given on Figure 3b is a good indicator of lithological transitions and accurately discriminates between the three layers observed at the uplifting of drilling debris (Reiffsteck et al., 2018).

2.3.1. Test at 11 m

Figure 4a and b show the pressure-volume diagram and evolution of pressure and volume as a function of time. In Figure 4a the blue curve is the pressure corrected for the hydrostatic effect and the inertia of the probe according to EN ISO 22476-4, the red curve is the creep. Five phases have been identified, the limits of which are shown in Figures 4a and b by numbers. On Figure 4b, the green curve (cell pressure) is the raw pressure exerted by the probe on the ground, the red curve is the volume injected and the blue curve is the pore pressure.

Phase 1: Between points 0 and 1, the volume of the probe varies little with the rise in pressure and the pore pressure is equal to the value obtained during the first stage. This is the pseudo-elastic phase of the test. In accordance with the theory in clays, soil deformation

takes place at constant volume with no variation in pore pressure.

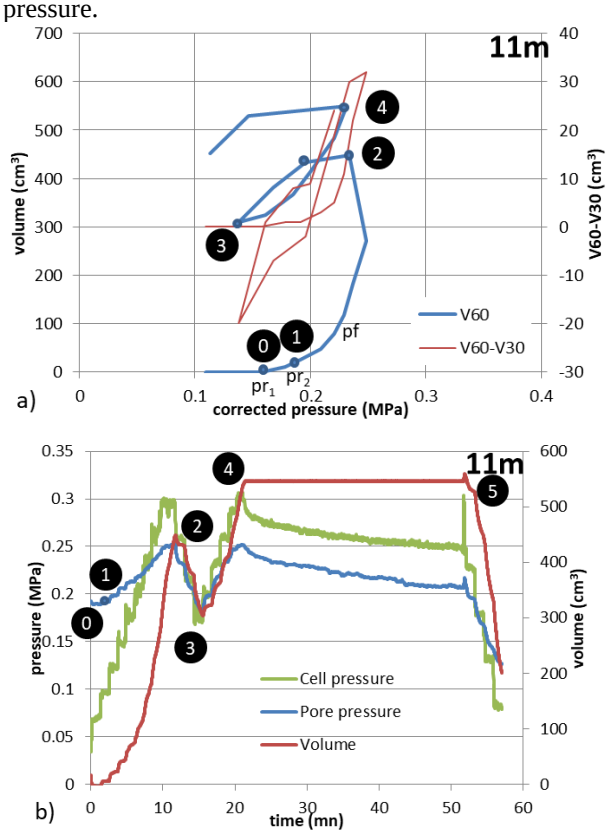

Figure 4. Results of PMTu test at 11 m depth (a) pressure-volume diagram (b) pressure and volume as a function of time

Phase 2: Between points 1 and 2, volume deformations are greater and increase step by step with an increase in pore pressure. This is the plastic phase.

Phase 3 and 4: Between points 2 to 3 and 3 to 4, these are the unloading-reloading stages. Pore pressures decrease during unloading and rise again during reloading (plastic phase stage).

Phase 5: Between 4 and 5: dissipation, volume and pressure are constant and pore pressure decreases. Beyond 5, unloading.

For this test, the plastic zone between 0 and 1 starts at a measured pressure of 0.17 MPa and the loading and unloading cycle is between the raw pressures of 0.17 and 0.3 MPa. The corrected dissipation pressure is p_c=0.23 MPa (raw pressure=0.3 MPa) for a creep pressure p_f=0.19 MPa.

It should be noted that in the slightly compact and disturbed ground in this test, the contact between the probe and the ground occurs at zero volume (deformation of the ground coming into contact with the probe until equilibrium pressure is reached). For these tests, creep during the 2Δt stage preceding the unloading and reloading cycle is very significant. In this case, p_{diss} is below the virgin curve giving the limit pressure p_ℓ. In this type of test, the soil has undergone a certain amount of disturbance (often unavoidable in AV2 soft clays).

2.3.2. Tests in clayey sands at 23m

The graphs for this test are given below in figure 5b. The representations are identical to those for the 11m test. The cycle phase (2-3 and 3-4) is located between point 0 and point 4. The loading-unloading cycle is therefore carried out in the elastic domain.

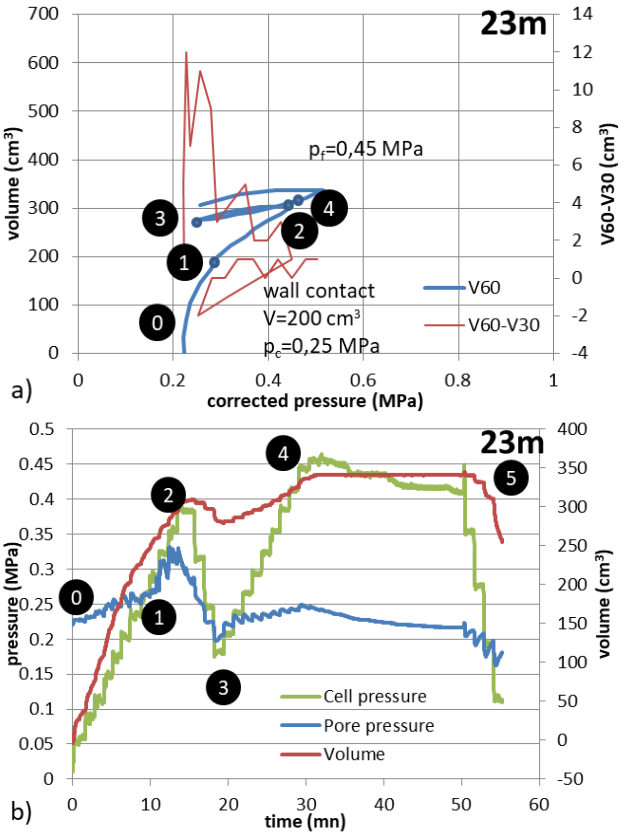

Figure 5. Results of PMTu test at 23m depth (a) pressure-volume diagram (b) pressures and volume as a function of time

However, between 0 and 2, the pore pressures (blue curve in Figure 5b) increased from 0.2 to 0.32 MPa. This may be explained by the existence of a disturbed zone around the probe. The probability of this hypothesis is strengthened by the fact that after the unloading loading loop, the pore pressure does not rise at point 4 to the same level as at point 2. We therefore have a rise in pore pressure from the first loading that dissipates between 2 and 4.

2.3.3. Dissipation tests

Figures 6a and b show the dissipation achieved from point 4 defined previously for the two tests discussed above.

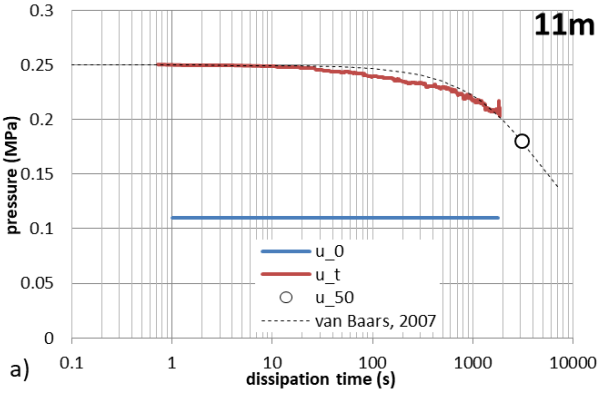

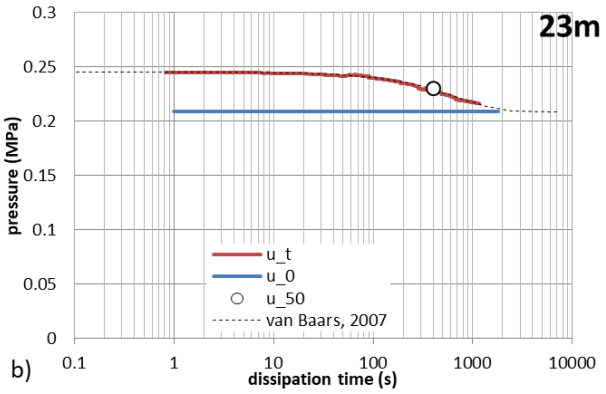

Figure 6. PMTu dissipation at (a) 11m and (b) 23 m

The pattern of dissipation is identical to that obtained with the piezocone. It should be noted that, as indicated by Reiffsteck et al (2002), when the t_{50} was not reached, it was extrapolated by the solution of the equation of Van Baars et al (2007). The t_{50s} obtained for all the tests ranged from 1,500 to 3,300 s in clays and from 1 to 400 s in clayey sands and sands.

2.4. Interpretation of tests

2.4.1. Stress path in clays

Figure 7 describes the stress paths during a test in soft clays.

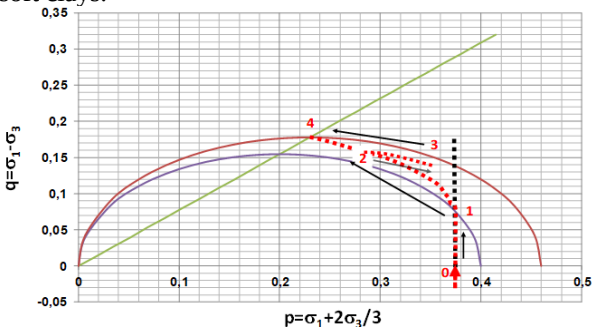

Figure 7. Stress path in soft clays

The notations are as follows: p'_{mi} mean effective pressure of loading stage i; u_i pore pressures at stage i; n_i and e_i are the porosity and void index of stage i respectively; $\Delta v/v$: volume variation of a unit element around the pressuremeter probe; β: volume compressibility of water (β varies with the gas content of the water) for pure water β=4.2. 10-4 MPa-1; p_ℓ* net limit pressure; m_v is the dimensionless loading modulus; m_{vr} is the dimensionless resurfacing modulus; S_u undrained soil cohesion.

Between 1 and 2, the loading is of the plastic type in the normally consolidated domain the deformation between 2 points is therefore:

$$\frac{\Delta v}{v0} = \frac{e_2-e_1}{1+e_1} = -\frac{Cc}{1+e_1}\cdot\left[log\left(\frac{p'_2}{p'_1}\right)\right] = \frac{1}{m_v}\cdot\left[log\left(\frac{p'_{m2}}{p'_{m1}}\right)\right] \quad (3)$$

pore pressure variation is u_2-u_1 with a porosity index variation is $\frac{n_2-n_1}{n_1} = -\gamma_w\cdot\beta\cdot(u_2-u_1)$. This can be written by expressing porosity as a function of void index $\frac{e_2-e_1}{e_1\cdot(1+e_2)} = -\gamma_w\cdot\beta\cdot(u_2-u_1)$ and if we assume a sufficiently small variation in void index so that $1+e_2$ is close to $1+e_1$ we then have

$$\frac{e_2-e_1}{(1+e_1)} = -\gamma_w\cdot\beta\cdot e_1\cdot(u_2-u_1) \quad (4)$$

We then have all calculations done between 1 and 2,

$$m_v = \frac{\gamma_w\cdot\beta.e_1.(u_2-u_1)}{\left[log\left(\frac{p'_{m2}}{p'_{m1}}\right)\right]} \quad (5)$$

With : $p'_{mi} = \left(\frac{2}{3}\cdot p'_i\right) + \frac{1}{3}\cdot\left(\gamma\cdot z_w + \gamma'\cdot(z-z_w)\right)$

Between 2 and 3, unloading is also of the plastic type in the overconsolidated domain. We then obtain by the same calculation:

$$m_{vr} = \frac{\gamma_w\cdot\beta.e_2.(u_3-u_2)}{\left[log\left(\frac{p'_{m3}}{p'_{m2}}\right)\right]} \quad (6)$$

In theory, these formulae could be used to calculate m_v and m_{vr}, provided that e_1 is known and the value of water compressibility β and material saturation are assumed. For the tests available, a determination of m_v and m_{vr}, using this method leads to a value for water β= $4.2.10^{-4}$ MPa^{-1} (total saturation) to very low values of m_v (10^{-6} to 10^{-7} MPa)) instead of 1.3 to 2.4 based on laboratory tests (volumic weight of the soil worth γ = 15 kN/m^3 tablecloth at 1 m below the TN). This discrepancy can be explained by an overestimation of the variation in u (underestimation of p'_{mi}) and/or by an underestimation of the compressibility of water, for example because insufficient account was taken of the presence of gas in the soil.

2.4.2. Drained and undrained moduli

Moduli on virgin curves and loops were determined in accordance with Reiffsteck et al (2022). The Ménard pressuremeter modulus is E_M (EN ISO 22476-4) and the drained modulus is E'_M. The undrained recharge modulus is E_R (NF P 94-110-2) and the drained modulus is E'_R. The calculation of the drained and undrained moduli is presented in Reiffsteck et al, (2022). Examination of E_M and is E'_Mconfirms that these two moduli are close. The ratios $E'_M/E_M$are thus between 0.8 and 1.08 (identical to within 20%). As E_M is measured in the elastic domain without any variation in pore pressure, we can consider that tests where E'_M/E_Mdiffers by more than 5% from 1 are disturbed with a true value of the pressuremeter modulus closer to E'_M. This value is called $E_{M\text{corrected}}$. With regard to the $E_R/E_{M\text{corrected}}$ ratios, we have 2 types of behaviour: in AV2 soft clays, $E_R/E_{M\text{corrected}}$ is dispersed and ranges from 0.91 to 1.65, with an average of 1.32 and a standard deviation of 0.6, which is much lower than the literature values ($E_R/\ E_M$ = 3 to 4 in Combarieu et al., (2001)). These tests are represented by the 11m test given above. In these tests, where E_R is measured in the plastic domain and with a pressure range greater than the E_M measurement range, the E'_R/E_R ratios are of the order of 2. In alluvial sandy-clay soils (As3) and in alterites, the $E_R/E_{M\text{corrected}}$ ratios are 3 to 6, which is in line with the literature.

3. Correlation with other tests carried out

3.1. Boreholes in the vicinity

The boreholes in the vicinity of the pressuremeter borehole (SPCYD-20) are the pressuremeter borehole

SP2D-20 with pressuremeter tests up to 30m; 5 piezocone tests PS3D-20, PS5D-20, PS6D-20, PS11D-20, PS12D-20 and a field vane profile. It should be noted that according to the Savatier et al. method (2012), the piezocones show that the AV2 soils are normally consolidated. Table 1 shows the position of these holes with reference to SPCYD-20:

Table 1. Soundings in the vicinity of SPCYD-20

Sounding	SP2D-20	PS12D-20	PS05D-20	PS06D-20	PS03D-20	PS11D-20	SCi2D20
X	348887,77	348890,37	348890,73	348909,30	348866,32	348870,25	348870,25
Y	541897,41	541897,92	541896,13	541879,11	541927,75	541931,30	541932,30
Z	2,36	2,35	2,35	2,27	1,87	1,83	1,83
Dist. (m)	0.82	1.84	2.52	27.67	37.60	38.49	39.37

3.2. S_u/q_t and S_u/p_ℓ^* correlations

Figure 8 shows the total peak cone resistance $q_t = q_c + (1-0{,}81)\cdot u_2$ as a function of the undrained cohesion S_u and the correlations between the net limit pressure and S_u (u_2 is the pore pressure measured at the base of the piezocone cone).

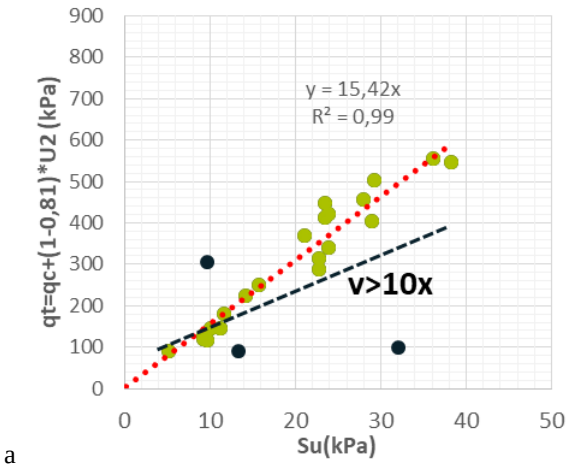

a

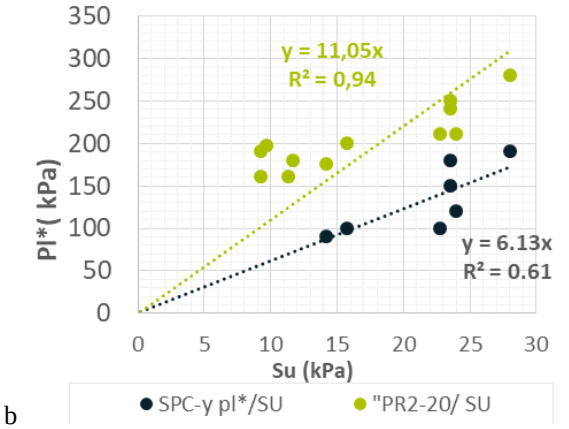

b

Figure 8. Correlations of S_u with penetration resistance and tests carried out with measurement of u

If we exclude 3 points corresponding to layer boundaries and sandy anomalies, we obtain an excellent correlation with: $q_t = 15{,}4 \cdot S_u$ i.e. $S_u = q_t/15{,}4$ with a correlation coefficient R^2=0.99. For limit pressures, the correlations are different for SP2D-20 and SPCYD-20. For the SP2D-20 test, the correlation deviates from what is generally found in soft clays with a slight dispersion of R=0.94. For SPCYD-20, we have $p_\ell^* = 6{,}13 \cdot S_u$ (instead of p_ℓ^* =5.5·S_u for p_ℓ^* <0.3 MPa from the literature) and a low dispersion (R=0.97). These correlations show a better quality of the pressuremeter tests with pore pressure measurement compared to the pressuremeter tests already carried out in SP2D-20.

3.3. Correlation between t_{50} derived from CPTu and PMTu

Figure 9 shows the dissipations of the PS12D20 piezocone at 10 m (AV2) and 22 m (AS3).

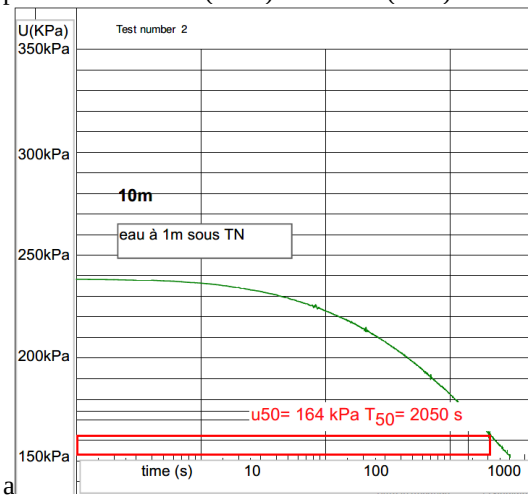

a

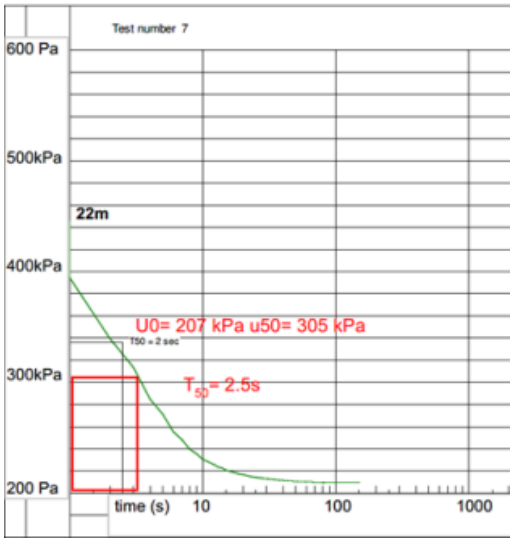

b

Figure 9. CPTu dissipation tests for PS12D20 at 10 and 22m

Figure 10 shows the correlation between the t_{50} measured at PMTu and at the piezocones located within a 27m radial distance of this borehole.

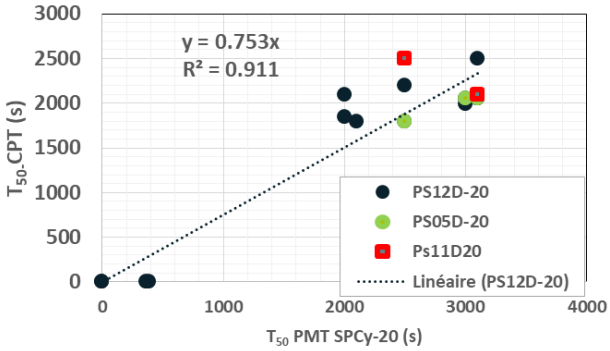

Figure 10. Correlation between PMTu SPCYD-20 and piezocones

The correlation between the 2 types of dissipation is excellent, with:
Tests in AS3 sands: t_{50} CPT= 0.753. t_{50PMTu} R^2=0.97
Tests in AV2 soft clays: 0.76. t_{50}CPT= t_{50PMTu} R^2=0.98

4. Comparison with laboratory tests and earthworks instrumentation

As the AV2 soils are normally consolidated, we will compare them with the radial odometer tests by applying a coefficient of 0.15 to the C_r values obtained from the in situ tests, as prescribed by Campanella et al (1998) for this type of soil. We will also apply a reduction coefficient of 0.76 to the Cr values estimated from the PMTu SCPYD-20 pressuremeter borehole, in accordance with the above correlation.

Figure 11 shows the C_r values estimated in this way according to Baligh and Levadou in Lunne et al (1997), compared with the available radial odometer tests (we have adjusted the altitude of the first test at PSD05-20 to take account of the variations in facies observed elsewhere).

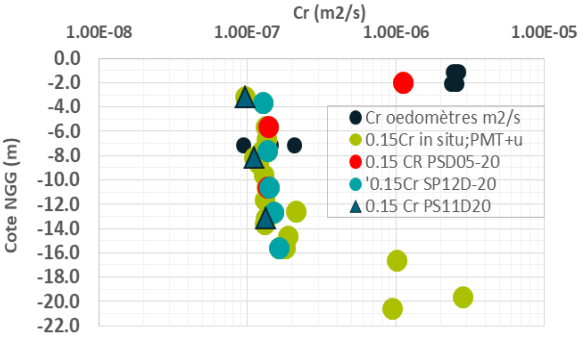

Figure 11. Cr comparison of in situ oedometers

The correspondence between radial drainage oedometer tests and in situ tests is good in sandy clays down to -2.5 NGG: laboratory C_r=2.6.10-6 m^2/s with in situ C_{rin} =1.12.10-6 m2/s. It is good in the characteristic AV2 clays from -2.5 to -16 NGG: laboratory C_r= 1 to 2.10-7 m^2/s and in situ C_r =0.98 to 2.12.10-7 m^2/s.

Measurements of consolidation settlement rate during instrumentation while the embankments are rising show an average correspondence with these results: C_r=3.2 to 3.5.10-8 m^2/s. This difference of a factor of 3 is probably explained by the difficulty of estimating the initial settlement during instrumentation in normally consolidated soil.

5. Conclusion

Pressuremeter tests with pore pressure measurements make it possible to detect the anomaly constituted by a variation in pore pressure during the pseudo-elastic phase and thus to correct the Menard pressuremeter modulus in this case. Correlations with undrained shear strength measurements show that pressuremeter tests with pore pressure measurements are of better quality than conventional tests. The pore pressure dissipations are close to those obtained in the immediate vicinity of the piezocone tests, and for the AV2 clays there is a close correlation: 0.76.t_{50CPT} = t_{50PMTu} correlation coefficient R^2=0.98. After applying this correlation and the correction proposed by Campanella et al (1998), the correlation with the instrumentation is acceptable, given the uncertainties in interpreting the instrumentation in normally consolidated soils and the possible disturbance during sampling and laboratory testing.

Acknowledgements

The project presented in this article is supported by Directorate-General for Territories and the Sea in French Guiana, French Republic.

References

Campanella R.G. (1998) Interpretation and use of piezocone test data for geotechnical design, presses de l'UBC,

Cassan M. (1987), Les essais in situ en mécanique des sols T.1. Ed. Eyrolles pp. 515- 520. (in French)

Cassan M. (2005) Essais de perméabilité sur site dans la reconnaissance des sols, pp 95-103. (in French)

Combarieu O., Canepa Y. ; (2001). L'essai cyclique au pressiomètre, BLPC pp.37 à 43. (in French)

Karagiannopoulos P.G., Peronne M., Reiffsteck P., Szymkiewicz F., (2019), Measure of the pore water pressure during expansion tests - physical and numerical approach, Proc. XVII ECSMGE, Reykjavic, ISBN 978-9935-9436-1-3

Karagiannopoulos P.G, Peronne M., Dang Q.H., Reiffsteck P., Benoît J., (2020) Cyclic pressuremeter tests with pore pressure measurements, application to CSR evaluation, 6th Int. Conf Geotechnical and Geophysical Site Charac., Budapest Hongrie, 8 pages

Lunne T., Powell J.J.M., Robertson P.K., (1997) Cone penetration testing in geotechnical practice CRC Press, 352 pages ISBN 9780419237501

Reiffsteck P., Savatier V., Karagiannopoulos P.G., et al., (2022). Essais d'expansion pressiométriques avec mesure de pression interstitielle- application au site du Larivot.JNGG 2022 (in French)

Reiffsteck P., Benoît, J., Bourdeau, C., Desanneaux G. (2018) Enhancing the geotechnical model using drilling parameters, J. Geotech. Geoenviron. Eng., Vol. 144, Issue 3, https://doi.org/10.1061/(ASCE)GT.1943-5606.0001836

Savatier V., Deluzarche R., Esteule I., Miralles J.-F., Lecoeur M., (2012) Variation du terme de pointe pénétrométrique avec la profondeur et détermination des paramètres de consolidation du sol. JNGG 2012 (in French)

Savatier V., Savatier M. (2016) Stress path during pressuremeter test and link between shear modulus and Menard pressuremeter in unsaturated soil, E-Unsat2016, http://doi.org/10.1051/e3sconf/20160909010